Article

Dual Effect of Secondary Solutes on Binding Equilibria: Contributions from Solute−Reactant Interactions and Solute−Water Interactions

Daryl K. Eggers,* Jennifer M. Le, Nhi T. Nham, Duc N. Pham, and Bria M. Castellano
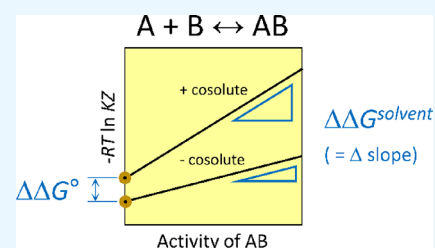
Read Online

ACCESS | Metrics & More | Article Recommendations | SI Supporting Information

ABSTRACT: This study examines the role of water in binding equilibria with a special focus on secondary solutes (cosolutes) that influence the equilibrium but are not constituents of the final product. Using a thermodynamic framework that includes an explicit term for the release of water molecules upon binding, this investigation reveals how solutes may alter equilibria by changing the activity of the reactants, reflected in $\Delta G^{\circ(obs)}$, and by changing the chemical potential of the solvent, reflected in ΔG^S. The framework is applied to four experimental binding systems that differ in the degree of electrostatic contributions. The model systems include the chelation of Ca^{2+} by EDTA and three host−guest reactions; the pairings of *p*-sulfonatocalix[4]arene with tetramethylammonium ion, cucurbit[7]uril with *N*-acetyl-phenylalanine-amide, and *β*-cyclodextrin with adamantane carboxylate are tested. Each reaction pair is examined by isothermal titration calorimetry at 25 °C in the presence of a common osmolyte, sucrose, and a common chaotrope, urea. Molar solutions of trehalose and phosphate were also tested with selected models. In general, cosolutes that enhance binding tend to reduce the solvation free energy penalty and cosolutes that weaken binding tend to increase the solvation free energy penalty. Notably, the nonpolar−nonpolar interaction between adamantane carboxylate and *β*-cyclodextrin is characterized by a ΔG^S value near zero. The results with *β*-cyclodextrin, in particular, prompt further discussions of the hydrophobic effect and the biocompatible properties of trehalose. Other investigators are encouraged to test and refine the approach taken here to further our understanding of solvent effects on molecular recognition.

$A + B \leftrightarrow AB$

$-RT \ln KZ$

+ cosolute

− cosolute

$\Delta\Delta G^S$

$\Delta\Delta G^{solvent}$ (= Δ slope)

$\Delta\Delta G^{\circ}$

Activity of AB

INTRODUCTION

The stable binding of two molecules or surfaces to form a binary complex is fundamental to many processes in the biophysical sciences. Of concern, the classical thermodynamic equations for binding equilibria in solution may be obscuring a complete understanding of this most basic phenomenon. Assuming that solvent molecules play an energetic role in the overall reaction thermodynamics and assuming that the binary complex interacts with fewer solvent molecules than the free reactants, the classical relationship for binding equilibria in solution must be viewed as originating from an unbalanced reaction.

In 2013, Castellano and Eggers first suggested a modified equation for binding equilibria that includes an explicit term for the change in solvent energy that accompanies formation of a noncovalent complex.[1] The thermodynamic framework, further elaborated in 2020,[2] includes a chemical potential for the subset of water molecules that are altered by the reaction, before and after complex formation. This modification captures the free energy change associated with the subset of water molecules that are released from the surfaces of the reactants upon binding. The proposed framework is summarized in eqs 1−8 below. For a binding reaction between two reactants, A and B, the following relationship is obtained for the change in reaction free energy:

$$\Delta G^{rxn} = RT \ln \frac{[AB]}{[A][B]} + [AB]\Delta G^S + \Delta G^{\circ} \quad (1)$$

where R is the gas constant, T is the temperature in kelvin, $[AB]$ is the concentration of binary complex, ΔG^S is the change in solvation free energy, and ΔG° is the standard-state free energy constant. In general, the value of ΔG^S reflects all linked reaction equilibria that are not explicitly included in the ratio of the products to reactants.

$$\Delta G^S = \sum \Delta G^{linked} = \Delta G^{solvent} + \sum \Delta G^{other} \quad (2)$$

With regard to eq 2, examples of other linked reactions include the transfer of a proton between a reactant and the buffer, monomer−dimer equilibria, and the binding or release of specific ions that accompany the formation of the complex. For the aqueous binding reactions in the current study, ΔG^S is expected to be dominated by the solvent-associated term,

denoted ΔG^{H2O} in our previous work, and defined by the following:

$$\Delta G^S = \Delta G^{solvent} = n(\overline{G}^{bulk} - \overline{G}^{surface}) \quad (3)$$

where "n" is the number of water molecules released per mole of complex formed, and where the bars above $\overline{G}^{bulk}$ and $\overline{G}^{surface}$ are a reminder that these represent location-averaged values for a water molecule in the bulk phase or next to a reactant surface, respectively. Using set theory terminology, bulk water is defined here as the complement to the solvation spheres of the reactants; bulk water includes the solvation spheres of all (nonreacting) cosolutes in addition to all water molecules that are distant from any surface. Because all solutes define a boundary with a solvation layer that may differ in energy from the average water molecule in the bulk phase, all secondary solutes will influence the value of $\overline{G}^{bulk}$ and, thereby, alter the value of ΔG^S. Thus, inclusion of the term $[AB]\cdot\Delta G^S$ in eq 1 enables one to account for changes in $\overline{G}^{bulk}$ due to cosolute–water interactions, an essential modification that opens a gateway to resolving other issues in physical chemistry and supramolecular chemistry.[3]

The standard-state free energy in eq 1, $\Delta G°$, is obtained from combining all of the constant terms in the derivation arising from the traditional reactants, leading to the following:

$$\Delta G° = (\mu^{°,AB} - \mu^{°,A} - \mu^{°,B}) + RT \ln \frac{\gamma_i^{AB}}{\gamma_i^A \gamma_i^B} - RT$$

$$\ln \frac{[AB]°}{[A]°[B]°} \quad (4)$$

where $\mu^{°,x}$ are the standard-state potentials, γ_i^x are the activity coefficients in solution i, and $[x]°$ are the reference concentrations of each species x. Note that γ_i^x and $[x]°$ are the constant terms for each reactant from the definition of thermodynamic activity, a_i^x:

$$a_i^x = \gamma_i^x \left(\frac{[x]_i}{[x]°} \right) \quad (5)$$

For a dilute (ideal) solution, the activity coefficients are set to unity and eq 4 reduces to the following:

$$\Delta G^{°(dilute)} = (\mu^{°,AB} - \mu^{°,A} - \mu^{°,B}) - RT \ln \frac{[AB]°}{[A]°[B]°} \quad (6)$$

For a concentrated (nonideal) solution, as relevant to the current study that employs secondary solutes in the molar concentration range, the activity coefficients will deviate from unity, and comparison of eq 4 with eq 6 leads to

$$\Delta G^{°(observed)} = \Delta G^{°(dilute)} + RT \ln \frac{\gamma_i^{AB}}{\gamma_i^A \gamma_i^B} \quad (7)$$

At equilibrium, $\Delta G^{rxn} = 0$, and eq 1 may be reduced to the following relationship:

$$\Delta G° = -RT \ln K - [AB]^{eq} \Delta G^S \quad (8)$$

With regard to eq 8, the equilibrium quotient, K, is defined as the ratio of the complex to free reactants at equilibrium in the direction of association. At infinite dilution, the last term in eq 8 approaches zero, and one obtains an equation familiar to most scientists. As with the classical approach, all concentrations are treated as dimensionless quantities due to division

by a reference concentration in the derivation, but the concentrations must be inserted in the same units. For reactions carried out in dilute solution, molarity is often used as the concentration unit. In the current study, for which the same reaction is observed in multiple solutions of high solute concentration, it is appropriate to convert molarity to molality (moles per kg of water). This conversion normalizes all results to the same mass of water and requires an accurate measurement of the solution density.

Previously, each model system in this study was tested against eq 8 in a dilute aqueous solution, and those results serve as the control experiments for the current investigation (Scheme 1).[1,4] Here, we expand on this experimental approach

Scheme 1. Model Binding Reactions
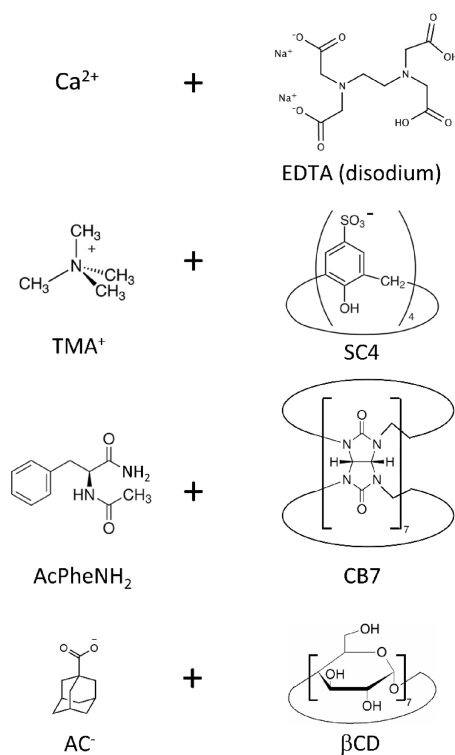
to demonstrate how secondary solutes influence the binding equilibrium by two distinct mechanisms, one that yields activity coefficients of nonunity and alters the observed value of $\Delta G°$ (due primarily to cosolute–reactant interactions) and one that yields a change in the solvation free energy (due to cosolute–water interactions).

■ MATERIALS AND METHODS

Reagents. Calcium chloride and disodium ethylenediaminetetraacetate (EDTA) were obtained from Fisher Scientific. Calcium and EDTA solutions were supplemented with 0.150 M 2-(4-morpholino)-ethanesulfonic acid buffer (MES) and adjusted to pH 6.2 at room temperature with a potassium hydroxide solution. Cucurbit[7]uril hydrate was purchased from Strem Chemicals (cat. no. 07-1325), and p-sulfonatocalix-[4]arene hydrate was obtained from TCI (cat. no. S0469). Stock solutions of CB7 and SC4 were titrated with 1.0 M KOH and brought up to the desired volume of solvent in 2.0 mM potassium phosphate buffer, pH 6.8–7.0. The dilution buffers for both SC4 and CB7 were supplemented with KCl to

account for potassium added during the stock neutralization step. The SC4 binding solutions contain 15 mM K$^+$ in total, and CB7 solutions contain 10 mM K$^+$ in total.[4] β-Cyclodextrin was obtained from Sigma-Aldrich (C4767) or TCI (C0777), and stock solutions of βCD were prepared in 2.0 mM potassium phosphate buffer (10 mM for the control in the absence of a cosolute). Tetramethylammonium chloride (TMA) was obtained from Fluka. Adamantane-1-carboxylic acid was purchased from Maybridge/Thermo Scientific, and AcPheNH$_2$ was obtained from Bachem Americas (cat. no. 4004733). Stock solutions of secondary solutes were made at room temperature from ultrapure water and the following reagents: urea (99%, Fisher), sucrose (99.9%, Fisher), trehalose (dihydrate, 99%, Acros), KH$_2$PO$_4$ (99.8%, Fisher), and K$_2$HPO$_4$ (99.5%, Fisher). The cesium phosphate solution was made by titrating phosphoric acid ($\sim$2 M) on ice with concentrated cesium hydroxide ($\sim$7 M, from Acros) until reaching pH 6.9, and then diluting with water to 1.0 M phosphate.

Methods. Density measurements were performed with a high-precision oscillating U-tube density meter (model DMA 5000, Anton Parr). The density meter was calibrated with air and ultrapure water, following the manufacturer's protocol. Molar concentrations were converted to molality through division by a correction factor, Z (kg H$_2$O per liter of solution), as calculated below:

$$Z = \rho_0 - \left(\frac{M_2 C_2 + M_3 C_3}{1000} \right) \tag{9}$$

where ρ_o is the density of the solution at 25.00 °C in g/mL (kg/L), $M_2 C_2$ refers to the formula mass and molar concentration of the secondary solute, and $M_3 C_3$ refers to the formula mass and molar concentration of the buffer. For the CB7 and SC4 solutions, the presence of KCl was also included in the last term for the calculations of Z.

Isothermal titration calorimetry was performed at 25 °C with a Microcal instrument, model VP-ITC (Malvern Panalytical), using the analysis programs provided by the manufacturer (Origin software). All solutions were degassed under a vacuum (ThermoVac). Prior to each calorimetry run, the sample cell (1.45 mL volume) was cleaned and rinsed with one volume of the same buffer solution. For Ca^{2+}/EDTA experiments, the sample cell was loaded with the EDTA solution, and the injection syringe was filled with CaCl$_2$ at a concentration 10-fold higher. For CB7 and SC4 trials, the host molecule occupied the sample cell and the injection syringe was filled with the guest molecule. In the case of βCD, the ITC locations were reversed with the guest molecule in the cell and βCD in the injection syringe. In a few cases for which the ITC c-factor <10, the concentration of the component in the syringe was increased to be 20-fold higher than the cell concentration.[5] The analog input range and reference power settings were adjusted in accordance with the sample concentrations and expected peak output for a given run. Typically, a series of 27 injections at 10 μL volume were used for starting cell concentrations of 0.10−1.00 mM, and 55 injections at 5 μL volume were employed for starting concentrations above 1.00 mM in the cell. For EDTA/Ca^{2+} at the highest concentration with 12.5 mM EDTA in the cell, the instrument was set for 106 injections of 2.5 μL each.[1] In all trials with all binding models, the first injection was set at 2 μL and the first titration peak was discarded from the analysis. The

stirring speed was increased from 307 to 351 rpm for the more viscous solutions of sucrose and trehalose. A control run, obtained by injecting the syringe component into a cell solution minus its binding partner, was subtracted from the binding experiment before analysis. Uncertainty in each K value is reported as the average error following multiple ITC trials at each condition ($n \geq 3$). The error in each free energy value was estimated by reanalyzing the slope of the corresponding lines when the maximum and minimum errors of each end point were used (at highest and lowest reactant concentration).

■ RESULTS

Previously, the utility of eq 8 was tested with multiple binding reactions in dilute solutions.[1,2,4] In each case, a straight line is obtained from the characteristic graph of $-RT\ln K$ versus the concentration of the complex, from which one may estimate ΔG° as the y-intercept and ΔG^S as the slope. As justified in a previous report, the concentration of the limiting reactant that occupies the ITC cell just prior to exceeding an equimolar ratio of injected reactant to binding partner in the cell is taken as the concentration of complex that corresponds to the computer-estimated value of the equilibrium quotient.[4]

To apply the same framework to solutions containing secondary solutes of a high concentration, a few modifications are appropriate. The first significant change is to convert all molar reactant concentrations to molality (moles per kilogram of water). This modification places all solutions on the same aqueous basis and has a negligible effect on the free energy values obtained from the control experiment performed in a dilute solution. For the concentrated solutions employed in this study, the density measurements and corresponding molality conversion factors (Z) are found in the Supporting Information, Table S1. Because calorimetry software typically requests input concentrations in units of molarity, the output (equilibrium quotient) from fitting the titration data also reflects the molar concentrations. To convert the molar-based equilibrium quotient, K, to a molality basis, each concentration in the equilibrium ratio expression must be divided by Z. For the generic binding reaction between A and B to form complex AB, the equilibrium quotient in units of molality is given by

$$\frac{\left(\frac{[AB]}{Z} \right)}{\left(\frac{[A]}{Z} \right)\left(\frac{[B]}{Z} \right)} = \frac{[AB]Z}{[A][B]} = KZ \tag{10}$$

Once the characteristic graph for eq 8 is plotted with units of molality, eq 7 is used to obtain the ratio of activity coefficients. To estimate an activity coefficient for the binary complex, one may define a general reaction coefficient (γ^{rxn}) that assumes all reactant activities are affected equally by the cosolute, as given by $\gamma^{rxn} = \gamma^A = \gamma^B = \gamma^{AB}$. This simplification is appropriate only when the cosolute does not interact preferentially with a reactant or product. For example, this assumption would be inappropriate for a case in which an ionic cosolute is added to a reaction involving a charged reactant species. Under conditions where the activity assumption is valid and the coefficients are equal, substitution into eq 7 leads to the following:

$$\Delta\Delta G^\circ = \Delta G^{\circ(obs)} - \Delta G^{\circ(dilute)} = RT \ln \left(1/\gamma^{rxn} \right) \tag{11}$$

Once γ^{rxn} has been estimated from eq 11, the concentration of the complex can be converted from molality to activity by
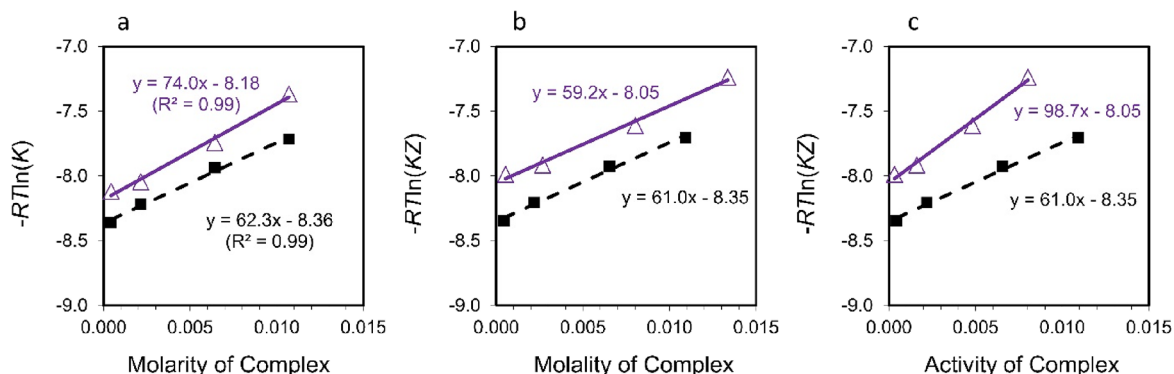
Figure 1. Steps in analyzing binding data for solutions of a secondary solute at high concentration. The control experiment is shown as a black dashed line, and the cosolute experiment is given by the purple solid line in each panel, accompanied by the corresponding linear fit. (a) K values obtained from ITC measurements are plotted as $-RT\ln K$ versus the molar concentration of complex at the 1:1 titration point in the calorimeter.[4] A linear fit indicates agreement with eq 8. (b) The concentration of the complex and the measured K value for each ITC trial are converted to units of molality. This alters both the x and y values for each (x, y) data point in the graph. At this stage, one calculates γ^{rxn} from the y-intercepts ($\Delta G°$) and eq 11. In this example, $T = 298.15$ K, $\Delta\Delta G° = +0.30$, and $\gamma^{rxn} = 0.60$. (c) The x-value of each data point is converted to thermodynamic activity by multiplying the molal concentration of the complex by the activity coefficient, γ^{rxn}. The slope of each line from this plot is ΔG^S for the reaction in the corresponding solution.

multiplication with γ^{rxn}. The sequence of steps in analyzing ITC data in the presence of molar cosolutes by this framework is depicted graphically in Figure 1.

The approach outlined by Figure 1 is applied first to the chelation of calcium cations by EDTA at pH 6.2. The control experiment for this model system in dilute solution was reported in 2013.[1] The aqueous solubilities of Ca^{2+} and EDTA allow this pairing to be tested over a wide concentration range, but a relatively high buffer concentration (150 mM MES) is recommended.[1] A value of pH 6.2 was selected for this reaction to maintain the binding quotient below 1×10^7, bypassing the need for a competitive inhibitor in ITC measurements. Solute selection for Ca^{2+}/EDTA binding was restricted to nonionic compounds to avoid direct interference with the charge–charge interactions of the reactants and to comply with the assumption behind eq 11. The Ca^{2+}/EDTA pairing was tested in three concentrations of urea, as well as 1.0 M solutions of sucrose and trehalose, as summarized in Figure 2. Note that the sample data in Figure 1 correspond to the control and 4.0 M urea data sets in Figure 2. All solution conditions yield a reasonable linear fit to eq 8, and the values of $\Delta G^{o(obs)}$ and ΔG^S follow in order from the least favorable binding solution (8 M urea, top line in Figure 2) to the most favorable solution (1 M sucrose, bottom line).

The next model binding system is the host–guest reaction of *p*-sulfonatocalix[4]arene (SC4) with a tetramethylammonium ion (TMA$^+$). The structure of SC4 may be described as a truncated cone with two hydrophilic rims that are separated by an aromatic midregion.[6] Because one rim of SC4 contains four negatively charged sulfonate groups at pH 7, this host tends to favor guest molecules with one or more positive charges.[7] As reasoned for the Ca^{2+}/EDTA system, only nonionic cosolutes were tested with this system to avoid interference with any interactions of opposite charge between the guest and host. As seen in Figure 3, sucrose at 1.0 M concentration increases the binding affinity of SC4/TMA$^+$ at infinite dilution (more negative $\Delta G°$) and decreases the solvation penalty (less positive ΔG^S) relative to the control experiment. Addition of 4.0 M urea, on the other hand, decreases the binding affinity and increases the solvation penalty relative to the control.
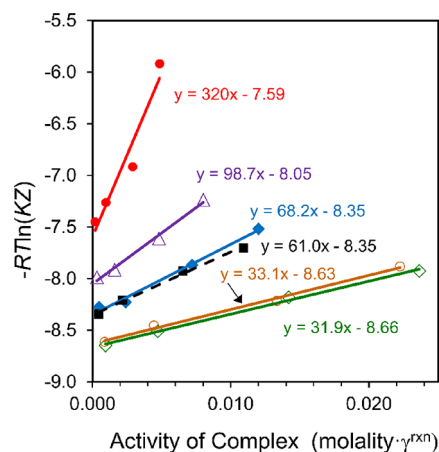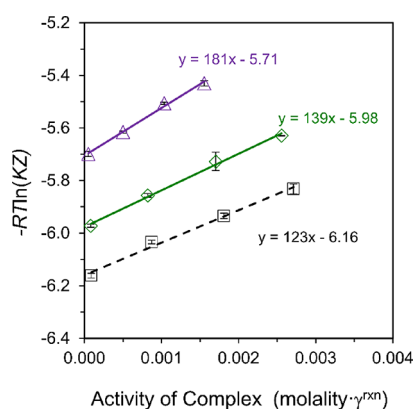

Figure 2. Binding analysis for Ca^{2+}/EDTA in the presence of secondary solutes at 25 °C. Solutions from top to bottom: 8.0 M urea (red circles), 4.0 M urea (purple open triangles), 2.0 M urea (blue diamonds), control (black squares, dashed line), 1.0 M trehalose (brown open circles), and 1.0 M sucrose (green open diamonds). The linear fit is given next to each line for which the slope corresponds to ΔG^S and the y-intercept is $\Delta G^{o(observed)}$. Error bars are approximately the same size as symbols but omitted for clarity.

The next binding investigation employs cucurbit[7]uril (CB7) as the host and modified amino acid, *N*-acetyl-phenylalanine-amide (AcPheNH$_2$), as the guest molecule. The structure of CB7 is a symmetrical ring with seven carbonyl oxygen atoms on each rim. This host tends to favor guest molecules with a positive charge, many of which have been tabulated.[8] CB7 has been shown to bind many amino acids with a preference for phenylalanine.[9,10] Previously, it was found that the carboxy-amidated form of this molecule binds too strongly to CB7 to measure reliably by ITC, so the positive charge was removed from the α-amino group by using an acetylated derivative.[4] The results, presented in Figure 4, deviate slightly from the trends of the previous two binding systems. The binding of CB7/AcPheNH$_2$ is weakest in the presence of 4.0 M urea, as expected, but the binding affinity was also reduced in the presence of 1.0 M sucrose relative to the control solution. The value of ΔG^S increased modestly
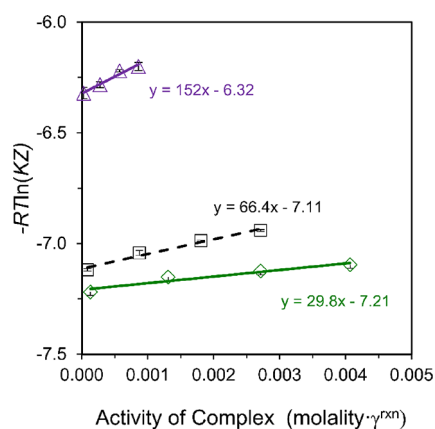
Figure 3. Binding analysis for SC4/TMA$^+$ in the presence of secondary solutes. Solutions from top to bottom: 4 M urea (purple, triangles), control (black squares, dashed line), and 1 M sucrose (green, diamonds). Error bars are shown, but small.
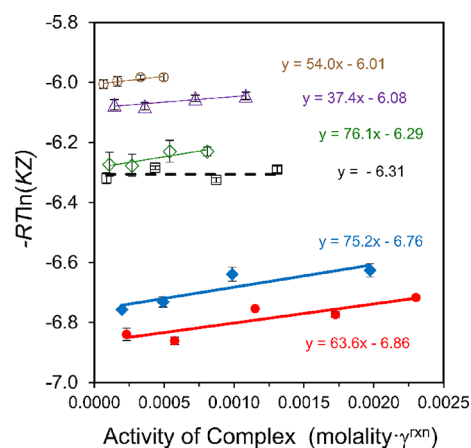

Figure 4. Binding analysis for CB7/AcPheNH$_2$ in the presence of secondary solutes. Solutions from top to bottom: 4 M urea (purple, triangles), 1 M sucrose (green, diamonds), and control (black squares, dashed line). Error bars are shown.

Figure 5. Binding analysis for βCD/AC$^-$ in the presence of secondary solutes. Solutions from top to bottom: 1.0 M trehalose (brown, open circles), 4.0 M urea (purple, open triangles), 1.0 M sucrose (green, open diamonds), control (black, open squares, dashed line), 1.0 M cesium phosphate buffer (blue, filled diamonds), and 1.0 M potassium phosphate buffer (red, filled circles). The horizontal line for the control indicates $\Delta G^S \approx 0$.

when the value in dilute solution (+120 kcal/mol) was compared to that in sucrose (+140 kcal/mol) and when the value in sucrose was compared to that in urea (+180 kcal/mol).

The final model system explores the interaction between the guest molecule, adamantane carboxylate (AC$^-$), and the host molecule, β-cyclodextrin (βCD), with intriguing results. As shown in Figure 5, the control solution yields a horizontal line, indicating that the change in the solvation free energy for this binding pair is near zero. The linear fits for all other solutions yield a small but positive slope. Small changes in solvation free energy appear to be a general feature of nonpolar interactions, although few examples have been characterized by this approach. A horizontal line in the characteristic plot for binding of a nonpolar bile acid with βCD has also been observed.[4]

Regarding the positive slope for the two phosphate solutions near the bottom of Figure 5, this result was not expected. Although the binding affinity increased relative to the control at all reactant concentrations, it was anticipated that 1 M phosphate might lower the average free energy of the bulk water and yield the first example of a favorable change in solvation free energy (negative value for ΔG^S). Phosphate is on the kosmotropic end of the Hofmeister series, which

corresponds to anions that stabilize protein structure.[11] In two related studies, the binding of adamantanol with βCD was enhanced slightly by the addition of 0.10 M phosphate,[12] and the binding of βCD with phenolphthalein followed the Hofmeister series upon addition of neutral salts.[13] An early hypothesis for the positive slope in Figure 5 was focused on the counterion of phosphate. If the positively charged counterions interact directly with the carboxylate group of AC$^-$, it might lead to a partially neutralized, less-polar guest molecule that binds with stronger affinity to βCD, especially at the lowest reactant concentrations tested where the excess in cation concentration is greatest. With this in mind, the buffer cation was switched from potassium to cesium because Cs$^+$ should interact less strongly with AC$^-$ in water due to its lower charge density relative to K$^+$.[14] However, 1.0 M cesium phosphate also resulted in a positive ΔG^S with a minor change in $\Delta G^{\circ(obs)}$, relative to the experiment in 1.0 M potassium phosphate (Figure 5). When the potassium phosphate concentration was lowered to 0.40 M to reduce the total ionic strength, the ΔG^S value was reduced slightly but still positive (Table S5).

■ DISCUSSION

Historically, secondary solute effects on biological equilibria have been interpreted most frequently by experimentalists who invoke the model of preferential interactions, as first introduced by Timasheff[15] and expanded by Record et al.,[16] or the model of osmotic stress, as promoted by Parsegian and co-workers.[17−19] Both of these models attribute solute effects to a nonhomogeneous distribution of the cosolute between the reactant surface and bulk phase. In contrast to the current work, the preferential interaction and osmotic stress models do not acknowledge that a solution may contain coexisting subpopulations of water that differ in their average chemical potential. The preferential interaction model completely omits any consideration for the effect of the cosolute (or reactant) on water, and although the osmotic stress model treats the chemical potential of bulk water as a solute-dependent variable, only one parameter is used to characterize all water molecules

Table 1. Summary of Results

model reaction	solution	linear fit (R^2)	$\Delta G^{o(obs)}$ (kcal/mol)	γ^{rxn}	ΔG^S (kcal/mol)
Ca^{2+}/EDTA	control	0.99	−8.35	1.00	+61
	2 M urea	0.99	−8.35	1.00	+68
	4 M urea	0.99	−8.05	0.60	+99
	8 M urea	0.94	−7.59	0.28	+320
	1 M trehalose	0.99	−8.57	1.45	+33
	1 M sucrose	0.99	−8.65	1.66	+32
SC4/TMA^+	control	0.98	−7.11	1.00	+66
	4 M urea	0.96	−6.32	0.26	+150
	1 M sucrose	0.93	−7.21	1.18	+30
CB7/AcPheNH$_2$	control	0.99	−6.16	1.00	+120
	4 M urea	0.99	−5.71	0.47	+180
	1 M sucrose	0.99	−5.98	0.74	+140
βCD/AC^-	control	(0.08)[a]	−6.31	1.00	∼0
	4 M urea	0.87	−6.08	0.68	+37
	1 M trehalose	0.86	−6.01	0.60	+54
	1 M sucrose	0.80	−6.29	0.97	+76
	1 M CsPhos	0.80	−6.76	2.14	+75
	1 M KPhos	0.79	−6.86	2.53	+64

[a]Poor fit supports $\Delta G^S = 0$.

in the system. Other possible issues with the models of preferential interactions and osmotic stress have been noted.[20]

One criticism of the thermodynamic framework presented in the current study originates from the statistical mechanics approach of Widom,[21,22] which has been cited as evidence that all water molecules in a given solution at equilibrium must have the same chemical potential, regardless of position.[23,24] We recognize the fact that there can be no change in energy for a system at equilibrium when a water molecule moves from one position to another position, for example, from a solute surface to the bulk. However, this requirement does not preclude a specific water molecule from encountering a change in free energy; it implies only that the change in energy of the water molecule under surveillance must be compensated by another water molecule that moves in the opposite direction, from the bulk to the surface. Solvent molecules are in a dynamic equilibrium, similar to the reactants and products of all reversible reactions at equilibrium. Thus, coexisting subpopulations of water that vary in chemical potential do not violate the fundamental laws of chemical equilibria.

Others may attribute the observed concentration dependence of K in a given solution to changing reactant activities due to self-interactions that increase with increasing concentration (e.g., reactant A with reactant A). The self-interaction hypothesis seems unlikely when one considers the reactant concentrations employed in our titration experiments. At a relatively high reactant concentration of 10 mM, for example, the ratio of water molecules to reactant molecules is approximately 55 to 0.010 M, or 5500:1, for a dilute aqueous solution. In a 4 M urea solution at the same reactant concentration, the corresponding ratio is about 4500:400:1 (water to urea to reactant). In both cases, reactant–reactant interactions should be rare compared to reactant–solvent interactions, and the activity coefficients of the reactants should remain constant for the concentration range employed here.

The current study proffers an alternative approach to solution thermodynamics that treats all solutes, large and small, as imposing a boundary condition that alters the chemical potential of adjacent water molecules. It is under-

stood that the time-averaged value of the chemical potential is identical for all water molecules in a given solution; all water molecules are sampling all surfaces over time in addition to the intervening space between solute molecules. However, at a given instant, the subpopulation of water molecules located next to each boundary may have a chemical potential significantly different from the bulk (time-averaged) value. Consequently, addition of a secondary solute will always shift the average free energy of the bulk phase toward the energy of the cosolute's hydration sphere, influencing the thermodynamics of any reaction in that defined solution.

In their treatise conveying the idea that the preferential interaction and osmotic stress models are analyzing the same phenomenon from different perspectives, Parsegian and co-workers stated that "the same (cosolute) molecule that binds to a protein also can directly affect protein conformation through changes in the activity of water".[18] We completely agree with this statement but contend that our approach is the only method that allows one to quantify and dissect the effect of the cosolute on water ($\Delta\Delta G^S$) from the effect of the cosolute on the reactants ($\Delta\Delta G^\circ$).

The thermodynamic parameters obtained from this study are summarized in Table 1. The linear fits to eq 8 are excellent for the first three model binding systems ($R^2 > 0.9$) but fall off slightly for the βCD/AC^- pairing ($R^2 \approx 0.8$). The weaker fits for βCD/AC^- may be due to the narrow concentration range employed for this pairing. Due to solubility limitations, the highest tested concentration for βCD/AC^- is ≤1.5 mM for each solution (Table S5).

In the case of urea solutions, a generalization can be made that urea decreases binding affinity and reduces γ^{rxn} for every model pairing. Also, the addition of urea increases the solvation penalty (yields a more positive ΔG^S) relative to the control for all models. Thus, urea exemplifies the dual effect that a cosolute may impose on binding equilibria via cosolute–reactant interactions and cosolute–water interactions.

The solute results for the two disaccharides, sucrose and trehalose, are less straightforward in interpretation than that for urea. For the Ca^{2+}/EDTA and SC4/TMA^+ model systems, sucrose was found to have a favorable effect on both ΔG° and

ΔG^S. On the other hand, sucrose had a slight destabilizing effect on binding for the pairings of CB7/AcPheNH$_2$ and βCD/AC$^-$. In a similar trend, trehalose was found to have a favorable effect on Ca^{2+}/EDTA binding but resulted in a significant reduction in the binding affinity of AC$^-$ with βCD (Table 1).

One explanation for the conflicting results with the disaccharide solutions is related to the variable contribution of electrostatic interactions in the model systems under comparison. Sugars are known to reduce the dielectric constant of aqueous solutions[25] and, therefore, should enhance binding events that involve charge—charge interactions such as the Ca^{2+}/EDTA and SC4/TMA$^+$ binding pairs. Urea, in contrast, is known to increase the dielectric constant and weaken charge—charge interactions,[26] consistent with the results in Table 1. Presumably, the effect of solute on the dielectric constant is reflected in the altered activity coefficients of the reactants relative to dilute solution, as embodied in γ^{rxn}. Thus, in the cases of sucrose and trehalose, cosolute—water interactions may influence both ΔG^S and $\Delta G^{o(obs)}$.

We also note that both disaccharides may have a preferential interaction with βCD over AC$^-$ because βCD is a carbohydrate synthesized from seven glucose units (Scheme 1). Thus, the assumption that all reactant activities are equally affected by sucrose or trehalose (eq 11) is unlikely to be valid for this binding model. A revised value for the activity coefficient of the complex between AC$^-$ and βCD would not alter $\Delta G^{o(obs)}$, but ΔG^S would be inversely proportional to the new value.

β-Cyclodextrin and the Hydrophobic Effect. The phenomenon known as the hydrophobic effect has a long and interesting history.[27] Of relevance to the current study, the interaction of nonpolar guest molecules with βCD has been touted as a model for the hydrophobic effect for many years.[28,29] The results in Figure 5 for binding of AC$^-$ to βCD lead us to suggest that the energetic contribution of the released water molecules that accompany a nonpolar—nonpolar interaction is very small, approaching zero in dilute solutions. This result conflicts with the viewpoint of others who maintain that the hydrophobic effect is driven by the release of high-energy water.[30−32] We concur with the idea that the water molecules adjacent to a nonpolar surface are higher in free energy than water near a polar surface, but the change in free energy upon release from the surface depends also on the time-averaged free energy of all (bulk) water molecules in the solution.[4]

These contrasting viewpoints are depicted schematically in Figure 6. The scenario for which the release of water favors the hydrophobic effect is represented by panel a, and the scenario suggested by the current work with βCD/AC$^-$ is represented by panel b. Note that the only difference between the two viewpoints is the position of the horizontal bar that denotes the bulk water free energy, a necessary benchmark for defining the change in solvation energy. In both scenarios, there exists a point where $\Delta G^S = 0$, labeled as the *aqua indifferens* point on the diagram. If the scenario depicted by Figure 6b is correct, then the energetics of nonpolar—nonpolar interactions in water should be the same as nonpolar—nonpolar interactions in the gas phase, if it were possible to measure gas-phase equilibria at the same concentrations. Interestingly, a computational study reached a similar conclusion by using molecular dynamics simulations to compare the properties of *n*-alkanes in water and in an ideal gas.[33] If the current work and cited MD study represent valid measures of nonpolar—nonpolar interactions,
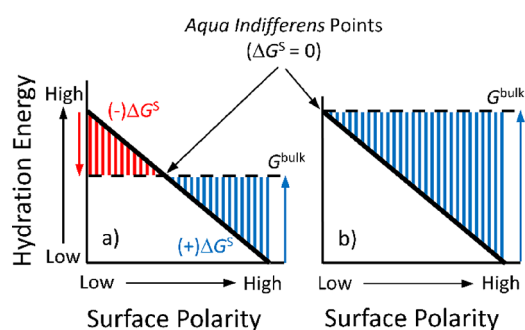
Figure 6. Raising the bar for bulk water in defining the change in solvation free energy. (a) Common view of solvation free energy for which the release of water from nonpolar solutes and surfaces is negative and favorable (red region) and release from polar solutes and surfaces is positive and unfavorable (blue region). At some intermediate point in polarity, there must exist a surface that corresponds to $\Delta G^S = 0$, labeled here as the *aqua indifferens* point. (b) Alternative view of solvation free energy in a dilute solution for which the value of G^{bulk} is raised (horizontal dashed line) until the change in solvation free energy for a surface of low polarity (i.e., hydrophobic surface) is near the *aqua indifferens* point. The ranking of hydration energies as a function of surface chemistry (diagonal line) is the same for both panels.

then one must conclude that the hydrophobic effect is driven by van der Waals interactions between nonpolar groups and not by a change in the free energy of water.

Regarding the unexpected results for βCD/AC$^-$ binding in phosphate solutions, this may be a situation where "other" linked equilibria are responsible for the sign and magnitude of ΔG^S (eq 2). Cyclodextrins have been reported to self-associate and form soluble clusters in water, as detected by several biophysical techniques including membrane permeation experiments.[34] If the phosphate's hydration sphere lowers the bar for G^{bulk} relative to a dilute solution, then clustering of βCD should be enhanced in phosphate solutions. In addition, because phosphate increases the nonpolar—nonpolar interaction between βCD and AC$^-$, it follows that phosphate should enhance the self-association of adamantane carboxylate, leading to a similar clustering effect for the other reactant. If true, then there exists a multimer—monomer equilibrium for each reactant cluster that contributes to the observed thermodynamics of binding. If the clustered state is favored energetically, then these linked equilibria may dominate over a negative value for $\Delta G^{solvent}$ (eq 2). Thus, in this case, the activity coefficients of the two monomeric (unclustered) reactants that lead to complex formation are viewed as constants with increasing reactant concentration, but reactant—self interactions are manifest in ΔG^S and increase with increasing reactant concentration, which weakens binding.

Conundrum of Trehalose. As stated earlier in this discussion, the favorable effect of trehalose on Ca^{2+}/EDTA binding may be due, in part, to a decrease in the dielectric constant of the bulk solution. But why did trehalose reduce the activity coefficients for binding of AC$^-$ to βCD, a pairing characterized by nonpolar—nonpolar interactions, and why did trehalose reduce formation of the complex to a greater extent than 4 M urea? Trehalose is a biocompatible osmolyte known to stabilize protein structure and enhance cell survival against environmental stresses, including drought.[35] Interestingly, trehalose is reported to have a minor impact on water structure,[36] and it has been difficult for experimentalists to

pinpoint any significant differences between aqueous solutions of trehalose and sucrose.[37]

In 1998, Singer and Lindquist were among the first to report the perplexing abilities of trehalose to stabilize proteins under thermal stress and, in another role, to suppress the aggregation of denatured proteins that remain unfolded.[38] Using a combination of experiments *in vitro* and *in vivo*, they concluded that the transient high concentration of trehalose following cellular stress must be reduced before the denatured proteins can refold with the help of molecular chaperones.

Using the model of preferential interactions as their experimental approach, Hong et al. concluded that trehalose has a favorable interaction with amide groups and a strong unfavorable interaction with hydrocarbons.[39] Thus, the ability of trehalose to suppress protein aggregation was attributed to its interactions with exposed peptide bonds, whereas its ability to stabilize the globular protein structure was attributed to its preferential exclusion from nonpolar surfaces upon unfolding (which favors the folded state by default).

In a relevant computational study, Paul and Paul used molecular dynamics to examine the self-association of neopentane (2,2-dimethylpropane) as a model for nonpolar interactions.[40,41] This investigation found that the association constant for the neopentane−neopentane interaction decreases with increasing trehalose concentration. Thus, the MD study concludes that trehalose weakens nonpolar−nonpolar interactions.

The reduced binding affinity of AC^- for βCD in 1 M trehalose, as observed in this work, aligns with the results of the neopentane study. Our finding suggests that trehalose reduces the aggregation of unfolded proteins by weakening the hydrophobic effect. Regarding the favorable effects of trehalose on thermal protein stability, we suggest that this property is directly related to the ability of trehalose to increase the chemical potential of the protein at surface residues corresponding to polar and charged groups, consistent with our observation that trehalose enhances the binding of Ca^{2+} to EDTA (Figure 2). Based on our limited data, sucrose should be as effective as trehalose in maintaining the folded state of a protein, but trehalose should be superior in preventing the aggregation of unfolded proteins.

Related Issues in Solution Thermodynamics. A quandary for the theories of preferential interactions and osmotic stress is their inability to explain the additive effects of multiple solutes. There are many reports in the literature that demonstrate how the effect of one solute may be enhanced or reversed by the addition of a second solute. Solutes that lead to offsetting effects are often referred to as "counteracting solutes" and play an important role in many marine organisms that accumulate high levels of urea as part of their normal metabolism.[35,42]

In a classic paper by von Hippel and Wong, the effects of guanidinium ion on the thermal stability of ribonuclease could be altered significantly by changing the counterion from chloride (denaturing) to thiocyanate (more denaturing) to acetate (less denaturing) to sulfate (stabilizing).[43]

Another highly investigated example of counteracting solute effects is the combination of urea and trimethylamine-*N*-oxide, or TMAO, a natural osmolyte.[42] The literature on TMAO solutions tends to emphasize changes in water structure, disrupted hydrogen bonding, and cosolute partitioning with no accounting for the change in solvent free energy. It is worth taking a pause here to reflect on the fact that all reaction

equilibria move toward the lowest free energy state of the system; therefore, if water is viewed as part of the system, then understanding the effect of solutes on the free energy of water seems a prerequisite to understanding the effect of solutes on binding and conformational equilibria, including protein folding.

The thermodynamic framework employed here, as encompassed in eqs 1−8, provides a means to rationalize the apparent additive effects of many solute combinations. Because the change in solvation energy depends on the average free energy of the bulk water molecules and because each specific solute should induce a unique solvation sphere of unique energy, the effect of multiple solutes on G^{bulk} (and ΔG^S, eq 3) should be additive. The additive property is expected to become less predictable with increasing total solute concentration as water molecules become a limiting factor in satisfying the solvation shell of every solute molecule.

Another issue in solution thermodynamics is the use of thermodynamic cycles that (attempt to) relate a reaction in the gas phase or in a reference solution to the same reaction in another solution containing a cosolute (Figure 7). The
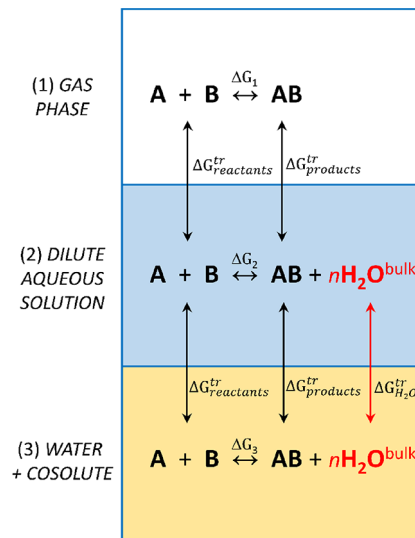
Figure 7. Inclusion of bulk water in thermodynamic cycles. The generic binding reaction defined in the gas (phase 1) is modified to acknowledge the release of a subset of water molecules when transferred to a dilute aqueous solution (phase 2). The change in chemical potential for this subset of water molecules is not captured by the transfer free energies of the reactants and products from the gas phase. When comparing the reaction in two aqueous solutions (phases 2 and 3), the transfer free energy for this subset of bulk water molecules should be included in the thermodynamic cycle (red arrow).

application and interpretation of thermodynamic cycles become muddled when the contribution of bulk water is included in the balanced reaction. Upon dissolution of reactants A and B from the gas phase (or from a solid phase), a subset of bulk water molecules is consumed to create the reactants' hydration spheres, and subsequent formation of the AB complex will release a fraction of the hydration waters back into the bulk solution. An adequate consideration for the gain in bulk water molecules upon complex formation is omitted from every thermodynamic cycle we encountered in the literature. This includes many studies that utilize the Tanford transfer model to analyze the effects of denatur-

ants,[44−46] neutral salts,[47] compatible osmolytes,[48] and macromolecular crowding agents[49] on protein structure and stability. Furthermore, if water is recognized as part of the balanced reaction in an aqueous reference solution, then a subset of water molecules must also be "transferred" to the solution of comparison to complete the thermodynamic cycle (Figure 7). Complicating things further, both $\Delta G°$ and ΔG^S are needed for each solvent phase if one wants to characterize the equilibrium at all reactant concentrations. Other issues, related to the use of solubility experiments to obtain the transfer free energies of model compounds and to estimate changes in protein stability, have been noted.[20]

Although eq 8 was derived with aqueous reaction equilibria in mind, the governing equation also has been applied to the formation of lanthanide container complexes in organic solvents.[50−54] Using NMR to obtain the equilibrium binding quotients at each titration point, Piguet and co-workers report that the ΔG^S values for their system are generally large in magnitude and favorable in sign. For example, a lanthanum complex formed in dichloromethane yields ΔG^S values of approximately −70 kcal/mol (−300 kJ/mol) for three different tridentate ligands, denoted L1−L3.[50] It should be noted that these titration experiments begin with the lanthanide ion prebound to three molecules of hexafluoroacetylacetonate (hfa) and one molecule of diglyme (dig). Typically, the thermodynamic analysis for these systems employs a conditional approach where excess diglyme is present in the solvent phase, allowing the concentration of unbound diglyme to be treated as a constant in the expression for the equilibrium quotient. We suggest that the subpopulation of diglyme that is released from the lanthanide upon ligand exchange defines a linked equilibrium that is embedded in the value ΔG^S. Diglyme is analogous to a water molecule in this study; the chemical potential of a diglyme molecule in the lanthanide complex should be significantly different than the potential of a diglyme molecule in the bulk solution. Thus, the lanthanide system may be a case where the favorable sign of ΔG^S is influenced by other linked equilibria in addition to the change in solvent free energy (eq 2).

CONCLUSIONS

This study is the first of its kind to analyze the effects of secondary solutes on model binding reactions with a governing equation that accounts for the participation of bulk water. Using this approach, it is possible to separate the effect of a cosolute on reactant activities from the effect of a cosolute on the free energy of bulk water, both of which contribute to the observed thermodynamics.

By selection of a set of model binding reactions that differ significantly in the degree of electrostatic interactions, it was discovered that some osmolyte effects are strongly dependent on the chemistry of the interacting surfaces. For example, trehalose addition was favorable for chelation of calcium ions by EDTA but unfavorable for the nonpolar−nonpolar interaction between adamantane carboxylate and β-cyclodextrin. Furthermore, the studies with AC$^-$/βCD suggest that the hydrophobic effect is characterized by relatively small changes in solvation energy, although few examples exist at this time.

While the sign and magnitude of ΔG^S may be influenced by other linked equilibria, as speculated for AC$^-$/βCD binding in molar phosphate solutions, the solvation energies reported here are believed to originate primarily from the water molecules that are released from the reactant surfaces upon complex formation. We encourage the scientific community to investigate other combinations of model binding systems and cosolutes by the experimental approach used here for the dual purpose of testing its utility and advancing our knowledge of solvent effects on molecular recognition.

■ ASSOCIATED CONTENT

Data Availability Statement

ITC data files underlying this study and the authors' response to manuscript reviews are openly available in the corresponding author's ScholarWorks page at https://works.bepress.com/daryl_eggers/.

Ⓢ Supporting Information

The Supporting Information is available free of charge at https://pubs.acs.org/doi/10.1021/acsomega.3c09329.

> Solution density measurements; table of equilibrium quotients, energies, and uncertainties for each model binding pair (PDF)

■ AUTHOR INFORMATION

Corresponding Author

Daryl K. Eggers − *Department of Chemistry, San José State University, San José, California 95192-0101, United States;* ⓞ orcid.org/0000-0003-1915-5945; Phone: 408-924-4960; Email: daryl.eggers@sjsu.edu

Authors

Jennifer M. Le − *Department of Chemistry, San José State University, San José, California 95192-0101, United States;* Present Address: Eikon Therapeutics, Hayward, California 94545, United States (J.M.L.)

Nhi T. Nham − *Department of Chemistry, San José State University, San José, California 95192-0101, United States;* Present Address: Guardant Health, Redwood City, California 94063, United States (N.T.N.)

Duc N. Pham − *Department of Chemistry, San José State University, San José, California 95192-0101, United States*

Bria M. Castellano − *Department of Chemistry, San José State University, San José, California 95192-0101, United States;* Present Address: Sarafan ChEM-H, Stanford University, Stanford, California 94305, United States (B.M.C.)

Complete contact information is available at: https://pubs.acs.org/10.1021/acsomega.3c09329

Author Contributions

The manuscript was written through contributions of all authors. All authors have given approval to the final version of the manuscript.

Notes

The authors declare no competing financial interest.

■ REFERENCES

(1) Castellano, B. M.; Eggers, D. K. Experimental support for a desolvation energy term in governing equations for binding equilibria. *J. Phys. Chem. B* **2013**, *117* (27), 8180−8188.

(2) Eggers, D. K.; Fu, S.; Ngo, D. V.; Vuong, E. H.; Brotin, T. Thermodynamic contribution of water in cryptophane host−guest binding reaction. *J. Phys. Chem. B* **2020**, *124* (30), 6585−6591.

(3) Cremer, P. S.; Flood, A. H.; Gibb, B. C.; Mobley, D. L. Collaborative routes to clarifying the murky waters of aqueous supramolecular chemistry. *Nat. Chem.* **2018**, *10* (1), 8−16.

(4) Eggers, D. K.; Brewer, A.; Cacatian, K. J.; Camat, L. A.; Castagnoli, D.; Chuang, N.; Chung, L. N.; Do, T.; Huynh, E.; Jenpichitkulchai, T.; Kaur, A.; Le, F.; Ong, R.; Pham, D.; Shao, K. Model binding experiments with cucurbit[7]uril and *p*-sulfonatocalix-[4]arene support use of explicit solvation term in governing equation for binding equilibria. *Supramol. Chem.* **2023**, *34* (2), 94−104.

(5) Tellinghuisen, J. Optimizing experimental parameters in isothermal titration calorimetry. *J. Phys. Chem. B* **2005**, *109* (42), 20027−20035.

(6) Perret, F.; Lazar, A. N.; Coleman, A. W. Biochemistry of the para-sulfonato-calix [n] arenes. *Chem. Commun.* **2006**, 2425.

(7) Guo, D.-S.; Wang, K.; Liu, Y. Selective binding behaviors of *p*-sulfonatocalixarenes in aqueous solution. *J. Incl. Phenom. Macrocycl. Chem.* **2008**, *62* (1), 1−21.

(8) Barrow, S. J.; Kasera, S.; Rowland, M. J.; del Barrio, J.; Scherman, O. A. Cucurbituril-based molecular recognition. *Chem. Rev.* **2015**, *115* (22), 12320−12406.

(9) Chinai, J. M.; Taylor, A. B.; Ryno, L. M.; Hargreaves, N. D.; Morris, C. A.; Hart, P. J.; Urbach, A. R. Molecular recognition of insulin by a synthetic receptor. *J. Am. Chem. Soc.* **2011**, *133* (23), 8810−8813.

(10) Lee, J. W.; Lee, H. H. L.; Ko, Y. H.; Kim, K.; Kim, H. I. Deciphering the specific high-affinity binding of cucurbit[7]uril to amino acids in water. *J. Phys. Chem. B* **2015**, *119* (13), 4628−4636.

(11) Collins, K. D.; Washabaugh, M. W. The Hofmeister effect and the behaviour of water at interfaces. *Q. Rev. Biophys.* **1985**, *18* (4), 323−422.

(12) Samuelsen, L.; Holm, R.; Schönbeck, C. Certain carboxylic acid buffers can destabilize β-cyclodextrin complexes by competitive interaction. *Int. J. Pharm.* **2020**, *589*, No. 119774.

(13) Buvári, Á.; Barcza, L. β-Cyclodextrin complexes of different type with inorganic compounds. *Inorg. Chim. Acta* **1979**, *33*, L179−L180.

(14) Collins, K. D. Charge density-dependent strength of hydration and biological structure. *Biophys. J.* **1997**, *72* (1), 65−76.

(15) Timasheff, S. N. Control of protein stability and reactions by weakly interacting cosolvents: The simplicity of the complicated. *Adv. Protein Chem.* **1998**, *51*, 355−432.

(16) Pegram, L. M.; Wendorff, T.; Erdmann, R.; Shkel, I.; Bellissimo, D.; Felitsky, D. J.; Record, M. T., Jr. Why Hofmeister effects of many salts favor protein folding but not DNA helix formation. *Proc. Natl. Acad. Sci. U. S. A.* **2010**, *107* (17), 7716−7721.

(17) Parsegian, V. A.; Rand, R. P.; Rau, D. C. Macromolecules and water: Probing with osmotic stress. In *Methods in Enzymology*; Academic Press, 1995; Vol. *259*, pp 43−94.

(18) Parsegian, V. A.; Rand, R. P.; Rau, D. C. Osmotic stress, crowding, preferential hydration, and binding: A comparison of perspectives. *Proc. Natl. Acad. Sci. U. S. A.* **2000**, *97* (8), 3987−3992.

(19) Harries, D.; Rau, D. C.; Parsegian, V. A. Solutes probe hydration in specific association of cyclodextrin and adamantane. *J. Am. Chem. Soc.* **2005**, *127* (7), 2184−2190.

(20) Eggers, D. K. A bulk water-dependent desolvation energy model for analyzing the effects of secondary solutes on biological equilibria. *Biochemistry* **2011**, *50* (12), 2004−2012.

(21) Widom, B. Structure of interfaces from uniformity of the chemical potential. *J. Stat. Phys.* **1978**, *19* (6), 563−574.

(22) Widom, B. Potential-distribution theory and the statistical mechanics of fluids. *J. Phys. Chem.* **1982**, *86* (6), 869−872.

(23) Ben-Amotz, D. Water-mediated hydrophobic interactions. *Annu. Rev. Phys. Chem.* **2016**, *67*, 617−638.

(24) Kantonen, S. A.; Henriksen, N. M.; Gilson, M. K. Accounting for apparent deviations between calorimetric and van't Hoff enthalpies. *Biochim. Biophys. Acta* **2018**, *1862* (3), 692−704.

(25) Malmberg, C. G.; Maryott, A. A. Dielectric constants of aqueous solutions of dextrose and sucrose. *J. Res. Natl. Bur. Stand.* **1950**, *45* (4), 299.

(26) Wyman, J., Jr. Dielectric constants: Ethanol—diethyl ether and urea—water solutions between 0 and 50°. *J. Am. Chem. Soc.* **1933**, *55* (10), 4116−4121.

(27) Southall, N. T.; Dill, K. A.; Haymet, A. D. J. A View of the hydrophobic effect. *J. Phys. Chem. B* **2002**, *106* (3), 521−533.

(28) Komiyama, M.; Bender, M. L. Importance of apolar binding in complex formation of cyclodextrins with adamantanecarboxylate. *J. Am. Chem. Soc.* **1978**, *100* (7), 2259−2260.

(29) Taulier, N.; Chalikian, T. V. Hydrophobic hydration in cyclodextrin complexation. *J. Phys. Chem. B* **2006**, *110* (25), 12222−12224.

(30) Griffiths, D. W.; Bender, M. L. Cycloamyloses as catalysts. In *Adv. Catal.*; Eley, D. D.; Pines, H.; Weisz, P. B., Eds.; Academic Press, 1973; Vol. *23*, pp 209−261.

(31) Biedermann, F.; Uzunova, V. D.; Scherman, O. A.; Nau, W. M.; De Simone, A. Release of high-energy water as an essential driving force for the high-affinity binding of cucurbit[n]urils. *J. Am. Chem. Soc.* **2012**, *134* (37), 15318−15323.

(32) Biedermann, F.; Nau, W. M.; Schneider, H.-J. The hydrophobic effect revisited—Studies with supramolecular complexes imply high-energy water as a noncovalent driving force. *Angew. Chem., Int. Ed.* **2014**, *53* (42), 11158−11171.

(33) Ferguson, A. L.; Debenedetti, P. G.; Panagiotopoulos, A. Z. Solubility and molecular conformations of *n*-alkane chains in water. *J. Phys. Chem. B* **2009**, *113* (18), 6405−6414.

(34) Loftsson, T.; Saokham, P.; Sá Couto, A. R. Self-association of cyclodextrins and cyclodextrin complexes in aqueous solutions. *Int. J. Pharm.* **2019**, *560*, 228−234.

(35) Yancey, P. H. Organic osmolytes as compatible, metabolic and counteracting cytoprotectants in high osmolarity and other stresses. *J. Exp. Biol.* **2005**, *208* (Pt 15), 2819−2830.

(36) Soper, A. K.; Ricci, M. A.; Bruni, F.; Rhys, N. H.; McLain, S. E. Trehalose in water revisited. *J. Phys. Chem. B* **2018**, *122* (29), 7365−7374.

(37) Olsson, C.; Swenson, J. Structural comparison between sucrose and trehalose in aqueous solution. *J. Phys. Chem. B* **2020**, *124* (15), 3074−3082.

(38) Singer, M. A.; Lindquist, S. Multiple effects of trehalose on protein folding in vitro and in vivo. *Mol. Cell* **1998**, *1* (5), 639−648.

(39) Hong, J.; Gierasch, L. M.; Liu, Z. Its preferential interactions with biopolymers account for diverse observed effects of trehalose. *Biophys. J.* **2015**, *109* (1), 144−153.

(40) Paul, S.; Paul, S. The influence of trehalose on hydrophobic interactions of small nonpolar solute: A molecular dynamics simulation study. *J. Chem. Phys.* **2013**, *139* (4), No. 044508.

(41) Paul, S.; Paul, S. Effects of the temperature and trehalose concentration on the hydrophobic interactions of a small nonpolar neopentane solute: A molecular dynamics simulation study. *RSC Adv.* **2014**, *4* (65), 34267−34280.

(42) Yancey, P. H.; Somero, G. N. Counteraction of urea destabilization of protein structure by methylamine osmoregulatory compounds of elasmobranch fishes. *Biochem. J.* **1979**, *183* (2), 317−323.

(43) von Hippel, P. H.; Wong, K. Y. On the conformational stability of globular proteins. The effects of various electrolytes and nonelectrolytes on the thermal ribonuclease transition. *J. Biol. Chem.* **1965**, *240* (10), 3909−3923.

(44) Nozaki, Y.; Tanford, C. The solubility of amino acids and related compounds in aqueous urea solutions. *J. Biol. Chem.* **1963**, *238*, 4074−4081.

(45) Tanford, C. Isothermal unfolding of globular proteins in aqueous urea solutions. *J. Am. Chem. Soc.* **1964**, *86* (10), 2050−2059.

(46) Robinson, D. R.; Jencks, W. P. Effect of denaturing agents of the urea-guanidinium class on the solubility of acetyltetraglycine ethyl ester and related compounds. *J Biol. Chem.* **1963**, *238*, PC1558−1560.

(47) Nandi, P. K.; Robinson, D. R. Effects of salts on the free energy of the peptide group. *J. Am. Chem. Soc.* **1972**, *94* (4), 1299−1308.

(48) Liu, Y.; Bolen, D. W. The peptide backbone plays a dominant role in protein stabilization by naturally occurring osmolytes. *Biochemistry* **1995**, *34* (39), 12884−12891.

(49) Zhou, H.-X.; Rivas, G.; Minton, A. P. Macromolecular crowding and confinement: Biochemical, biophysical, and potential physiological consequences. *Annu. Rev. Biophys.* **2008**, *37*, 375−397.

(50) Baudet, K.; Guerra, S.; Piguet, C. Chemical potential of the solvent: A crucial player for rationalizing host−guest affinities. *Chem. - Eur. J.* **2017**, *23* (66), 16787−16798.

(51) Baudet, K.; Kale, V.; Mirzakhani, M.; Babel, L.; Naseri, S.; Besnard, C.; Nozary, H.; Piguet, C. Neutral heteroleptic lanthanide complexes for unravelling host−guest assemblies in organic solvents: The law of mass action revisited. *Inorg. Chem.* **2020**, *59* (1), 62−75.

(52) Mirzakhani, M.; Nozary, H.; Naseri, S.; Besnard, C.; Guénée, L.; Piguet, C. Bottom-up approach for the rational loading of linear oligomers and polymers with lanthanides. *Inorg. Chem.* **2021**, *60* (20), 15529−15542.

(53) Naseri, S.; Mirzakhani, M.; Besnard, C.; Guénée, L.; Briant, L.; Nozary, H.; Piguet, C. Preorganized polyaromatic soft terdentate hosts for the capture of $[Ln(\beta\text{-diketonate})_3]$ guests in solution. *Chem. - Eur. J.* **2023**, *29* (10), No. e202202727.

(54) Le-Hoang, G.; Guénée, L.; Naseri, S.; Besnard, C.; Piguet, C. Metal template synthesis of 'broken' aromatic preorganized terdentate hosts for the recognition of lanthanide tris-β-diketonate guests. *Helv. Chim. Acta* **2023**, *106* (5), No. e202200190.